

General Disclaimer

One or more of the Following Statements may affect this Document

- This document has been reproduced from the best copy furnished by the organizational source. It is being released in the interest of making available as much information as possible.
- This document may contain data, which exceeds the sheet parameters. It was furnished in this condition by the organizational source and is the best copy available.
- This document may contain tone-on-tone or color graphs, charts and/or pictures, which have been reproduced in black and white.
- This document is paginated as submitted by the original source.
- Portions of this document are not fully legible due to the historical nature of some of the material. However, it is the best reproduction available from the original submission.

INVERSE TRANSONIC AIRFOIL DESIGN METHODS
INCLUDING BOUNDARY LAYER AND VISCOUS INTERACTION EFFECTS

(NASA-CR-158136) INVERSE TRANSONIC AIRFOIL
DESIGN METHODS INCLUDING BOUNDARY LAYER AND
VISCOUS INTERACTION EFFECTS Semiannual
Progress Report, 1 Aug. 1978 - 31 Jan. 1979
(Texas A&M Univ.) 16 p HC A02/MF A01

N79-17805

G3/02 Unclass
16322



**aerospace
engineering
department**

TEXAS A&M UNIVERSITY

SEMI ANNUAL PROGRESS REPORT
AUGUST 1, 1978 - JANUARY 31, 1979
(NASA GRANT No. NSG - 1174)



TAMRF REPORT No. 3224-79-01

LELAND A. CARLSON
ASSOCIATE PROFESSOR
TEXAS A&M UNIVERSITY
COLLEGE STATION, TX 77843

TEXAS ENGINEERING EXPERIMENT STATION

The NASA Technical Officer for this grant is Mr. J.C. South, Jr. Subsonic-
Transonic Aerodynamics Division, NASA Langley.

I. Introduction

This report covers the period August 1, 1978 to January 31, 1979. The primary task during this reporting period was the development of a fully conservative solution method and the incorporation of it into the TRANDES code. Wave drag and massive separation studies were also conducted.

II. Discussion of Research

A. Massive Separation Studies

As indicated in the last progress report, this effort is studying the application of the present model and method to the NASA 4412 Airfoil. Extensive experimental data, including pressure distributions, have been collected from the literature. Unfortunately, difficulty has been encountered in matching this data at low angles of attack to theoretical results obtained from the current code. Part of the problem was errors in the coordinate computation scheme, but this problem has been corrected and a $1/2^\circ$ angle of attack error still exists.

Comparison of the theoretical NASA 4412 ordinates with those used experimentally indicates some differences on the lower surface near the trailing edge. These discrepancies are small, however, and theoretical results using both sets only differ slightly. Thus the origin of the $1/2^\circ\alpha$ error is unknown; and it will for the time being be ignored in the interest of obtaining high angle of attack results. These latter results should be available shortly, will concentrate on determining input parameters for conventional airfoils, and will examine methods of drag calculation. This effort is being conducted by an undergraduate student.

B. Leading Edge & Wave Drag Studies

During this reporting period, work was initiated by an undergraduate to develop a leading edge grid imbedment scheme. Unfortunately, the student involved decided in December to accept a job offer and left abruptly. While

progress was made, the exact status of the work is currently being studied and will, hopefully, be reported later.

C. Fully Conservative Codes

The primary task during this reporting period has been the development and incorporation into TRANDES of a fully conservative analysis method utilizing the artificial compressibility approach. The present work closely follows Ref. 1 but allows for lifting cases and finite thickness airfoils and utilizes a stretched coordinate system. The solution scheme is a three level Richardson method for which has, in the present case, a stability requirement of

$$\left(\frac{\Delta t}{\Delta s}\right)^2 < \frac{w}{2(f_{LE}^2 + \alpha^2 g_{JB}^2)}$$

where	$0 < w < 2$	a "relaxation" like parameter
	$\alpha = \Delta s / \Delta \eta$	ratio of step sizes
	f_{LE}	maximum value of horizontal coordinate stretching factor
	g_{JB}	maximum value of vertical coordinate stretching factor

Initial results with the method indicated that the solutions trended to exhibit ski-ramp shocks. That is, the pressure just upstream of the shock wave would have large changes in dc_p/dx . This type of structure is shown on Figures 1 and 2 for NVIS = 1. Numerical experiments at TAMU and NASA Langley subsequently showed that this ramp behavior could be mitigated by increasing the artificial viscosity just upstream of the shock. In practice, this increase was accomplished by using for the artificial viscosity

$$\mu = 1 - (\alpha^2 / g^2)^{NVIS}$$

By increasing NVIS, μ would be increased.

Typical coarse and medium grid results using the NVIS concept are shown on Figures 1 and 2. Obviously, the solution is sensitive to NVIS and, as shown by Figure 2, the use of NVIS does not completely eliminate the ski-ramp structure. It should be noted that values of NVIS higher than two induced

for the medium grid cases numerical instability.

At this point it was suggested that the inclusion of ϕ_{xt} in the solution scheme might be of value. For the three-level scheme, the addition of ϕ_{xt} means that the governing equation is of the form

$$\bar{p} \phi_{xt} + \epsilon \bar{p} \phi_t + \bar{p} \delta \phi_{xt} = (\bar{p} u)_x + (\bar{p} v)_y$$

where $\phi_{xt} \sim (\phi_{ij}^n - \phi_{i-j}^n) - (\phi_{ij}^{n-1} - \phi_{i-j}^{n-1})$

Since the present method utilizes complete surface boundary conditions and hence thickness, the addition of ϕ_{xt} created some problems as to storing ϕ_{ij}^{n-1} values at boundary condition ghost points. The creation of a dummy array solved this problem, however; and the ensuing results did exhibit enhanced numerical stability.

Simultaneously, NASA Langley discovered that in the ACM formulation being used by TAMU that the artificial viscosity was being computed at the $(i+1/2, j)$ point instead of the (i, j) location. A simple fix was devised and typical results are shown on Figure 3. Surprisingly, the results were still sensitive to the value of NVIS and exhibited for some cases ski-ramp type shocks.

In spite of these subtle points, the method appeared to be working well. Thus, accuracy tests for various cases were conducted. For subcritical lifting and nonlifting cases, comparison was made with results from the TRANDES program. For $\alpha = 0^\circ$, $M_\infty = 0.6$, 6% biconvex, the new method, called CØNV3, yielded C_p results that agreed almost exactly with the TRANDES values.

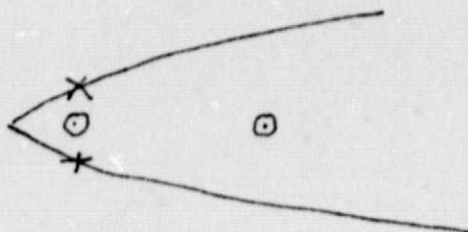
For lifting cases, such as $\alpha = 1^\circ$, $M_\infty = 0.6$, the aerodynamic coefficient agreement was excellent; but the TRANDES results showed C_p overshoot in the upper surface leading edge region which was not predicted by CØNV3. Subsequent investigation determined that this difference was due to the treatment of the (ILE-1, JB-1) point (see sketch).

J=JB

JB-1

ILE-1

I=ILE



The TRANDES code, which solves the full potential equation, needs to compute ϕ_{xy} at (ILE-1, JB-1) a ϕ value at (ILE,JB). This value is obtained by either satisfying the boundary condition at the lower surface (marked +) or at the upper surface (marked X). In TRANDES, the lower extropolation was selected since this approach yielded better answers, when compared to other methods, for the NACA 0012.

When the TRANDES program was run using the upper surface extropolation, the results agreed very well with CØNV3. Based upon this agreement, it was concluded that CØNV3 was accurate for subcritical cases, although subtle leading edge problems might still exist.

For supercritical cases, comparison was made with non-lifting results provided by NASA Langley. Initial comparisons are shown on Figure 4 for a 10% biconvex case. This case is difficult in that it has a trailing edge supersonic/supersonic shock; and, as can be seen, there is some disagreement between the two methods. However, the Langley results used a thin wing small perturbation boundary condition; while TAMU used the full boundary condition. When the CØNV3 code used thin airfoil small perturbation boundary conditions, the results shown on Figure 5 were obtained. Subsequent tests showed that the differences on Figure 4 were primarily due to usage of the full condition and that finite thickness only influenced the pressures slightly. In any event, it was concluded that CØNV3 an accurate code, and some lifting solutions were obtained.

At this time (mid December) results of research at NASA Langley by Jerry South, Jr. became available which determined the origin of the ski-ramp shock problem. As a result a new code, called MIDSEG, has been written. The difference, between CØNV3 and MIDSEG will be reported later. However, some

results, comparing the two codes are shown on Figures 6 and 7. Notice that the CONV3 results exhibit a slight ski-ramp shock and that the C_p distribution and shock location is grid size sensitive. On the other hand, MIDSEG does not have these features. As a result, the present effort is concentrating on the MIDSEG type approach.

III. Personnel

- (1) Leland A. Carlson, Associate Professor, Principal Investigator,
1/4 Time August, 1/8 Time September to present.
- (2) Paul Hagseth, Undergraduate Research Assistant, August 1978
to December 1978.
- (3) Mike Watts, Undergraduate Research Assistant, September 1978
to present.

IV. References

1. Hafa, M.M., Murman, E.M., and South, J.C., "Artificial Compressibility Methods for Numerical Solution of Transonic Full Potential Equation," AIAA Paper 78-1148, July 1978.

V. Acknowledgement

The Author gratefully acknowledges the assistance and aid of Jerry C. South, Jr., NASA Langley, in developing the ACM methods discussed in this report.

ORIGINAL PAGE IS
OF POOR QUALITY

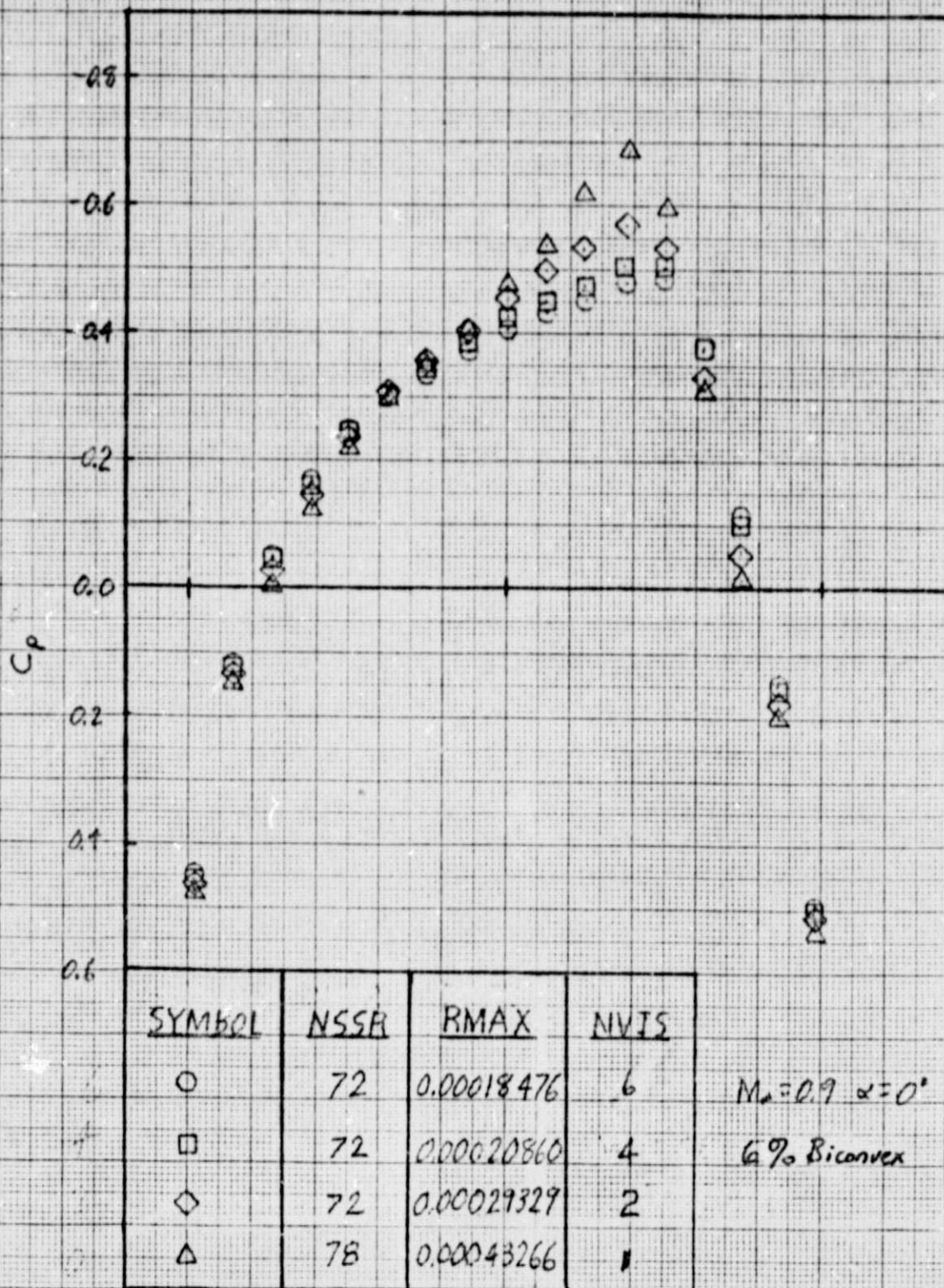


Figure 1. The Effect of NVIS On Coarse Grid Results

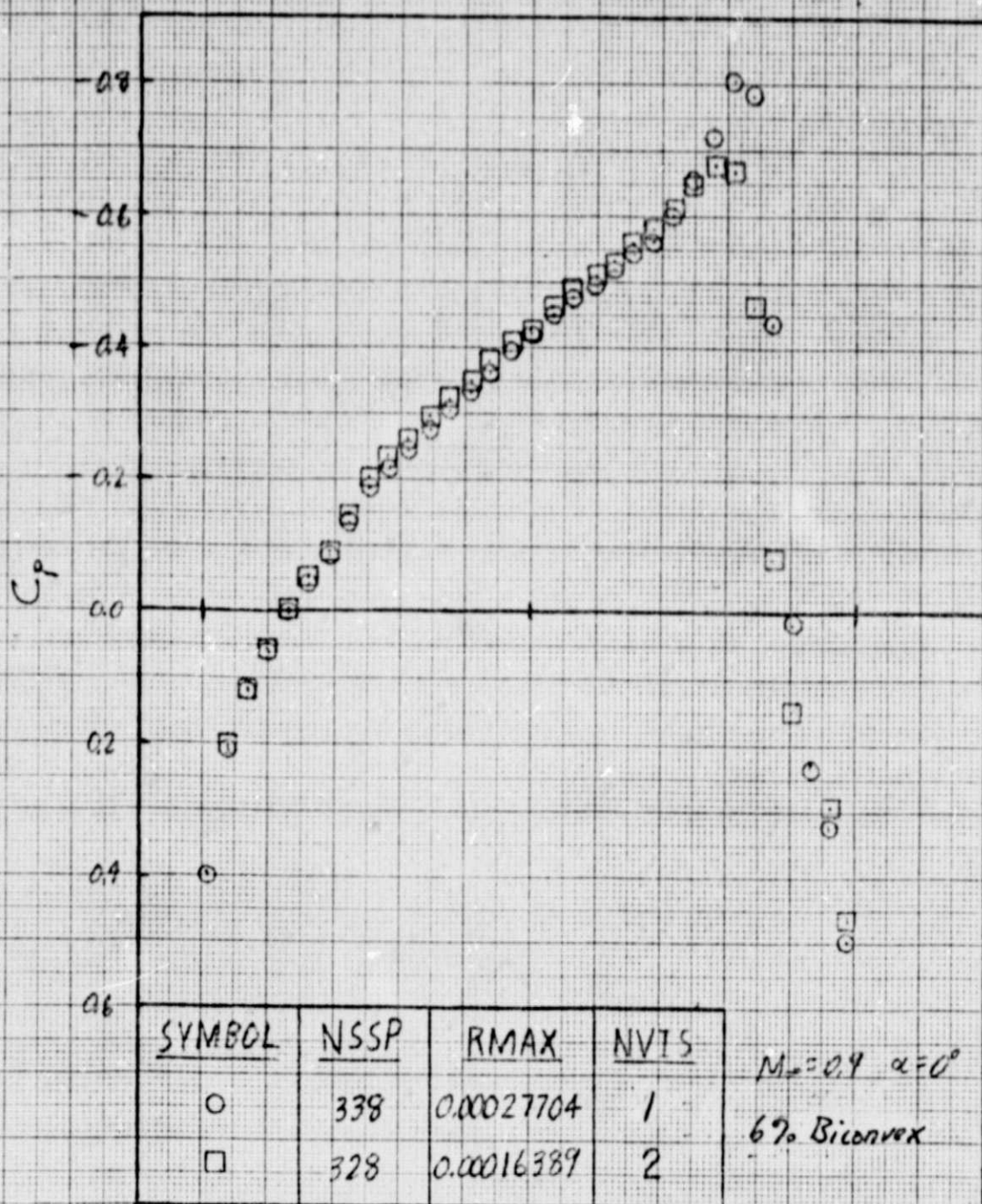


Figure 2. The Effect of NVIS on Medium Grid Results

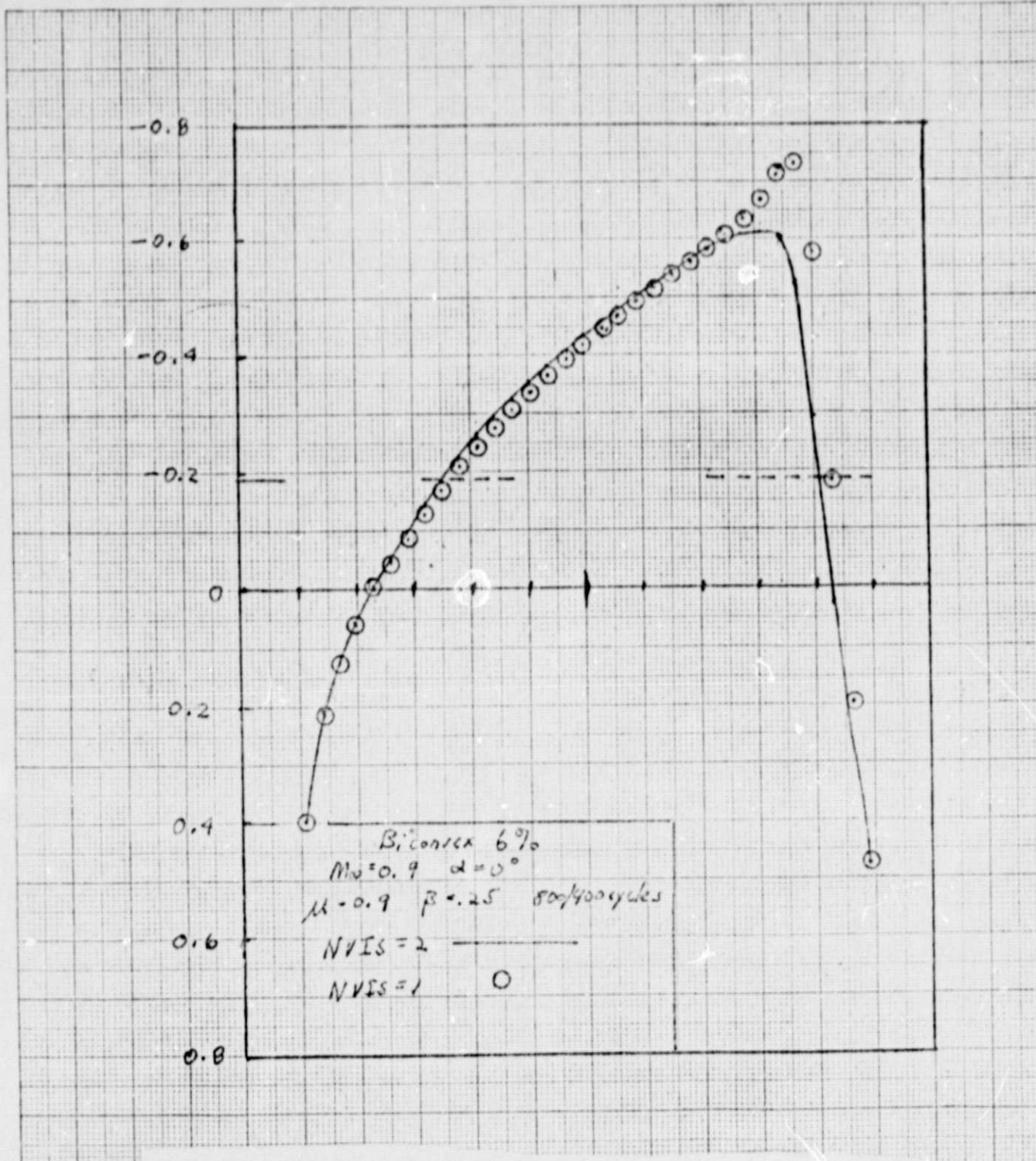


Figure 3. The Effect of NVIS With Correct μ Location

10/22/78

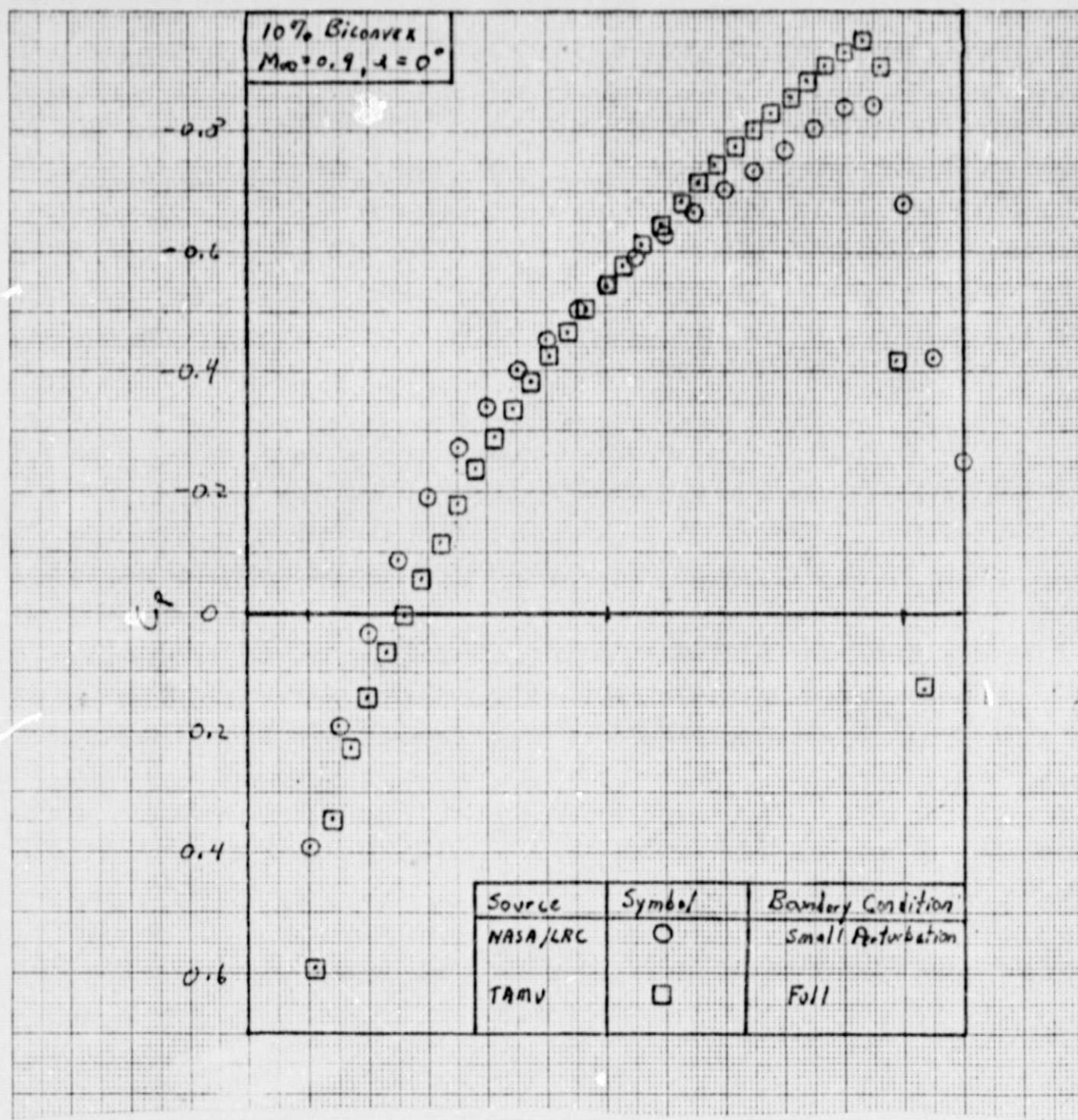


Figure 4. The Effect of Full vs. Small Perturbation Boundary Conditions.

11/29/78

ORIGINAL PAGE IS
OF POOR QUALITY

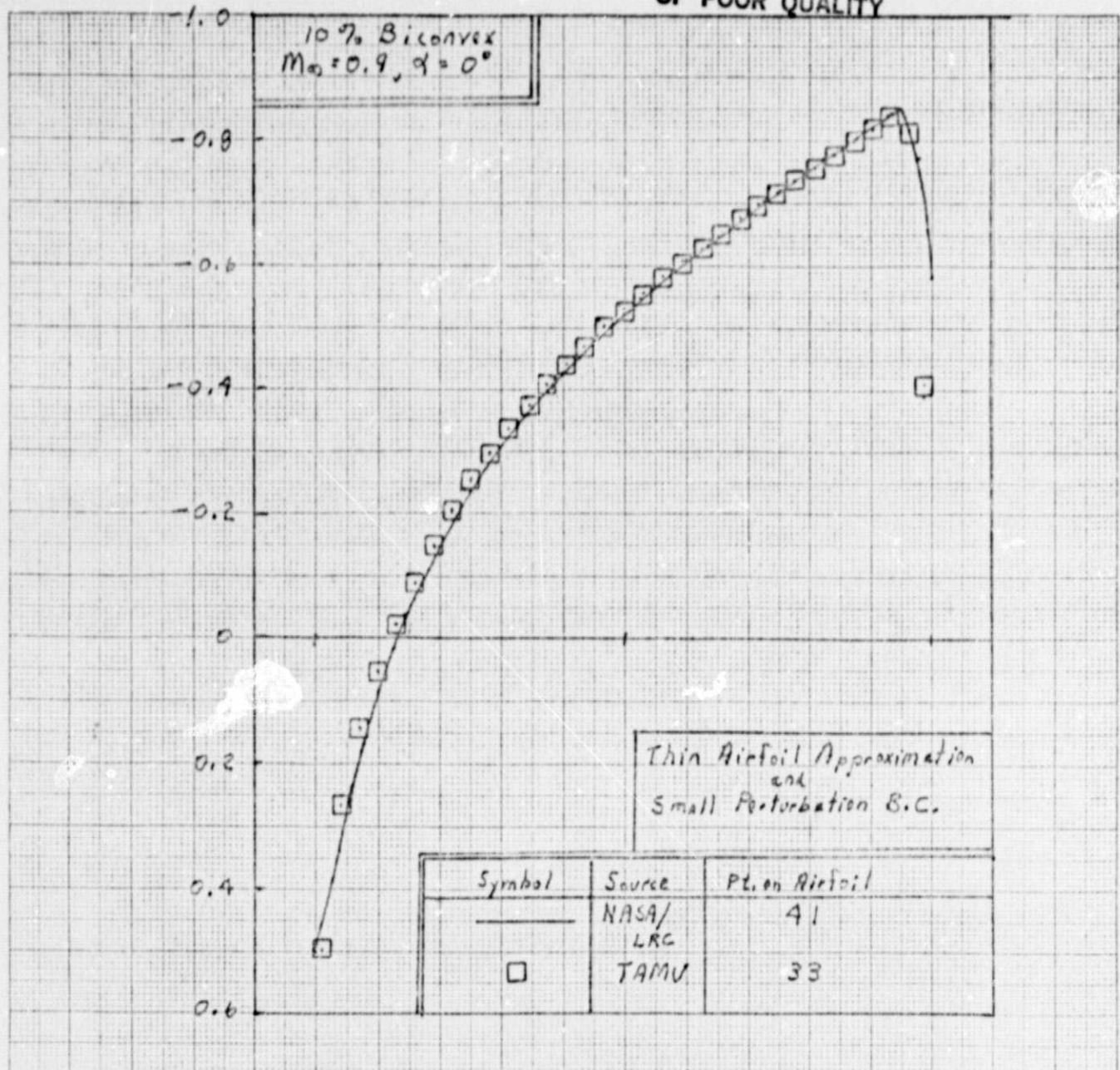


Figure 5. Comparison Of CONV3 Code Results with NASA Langley

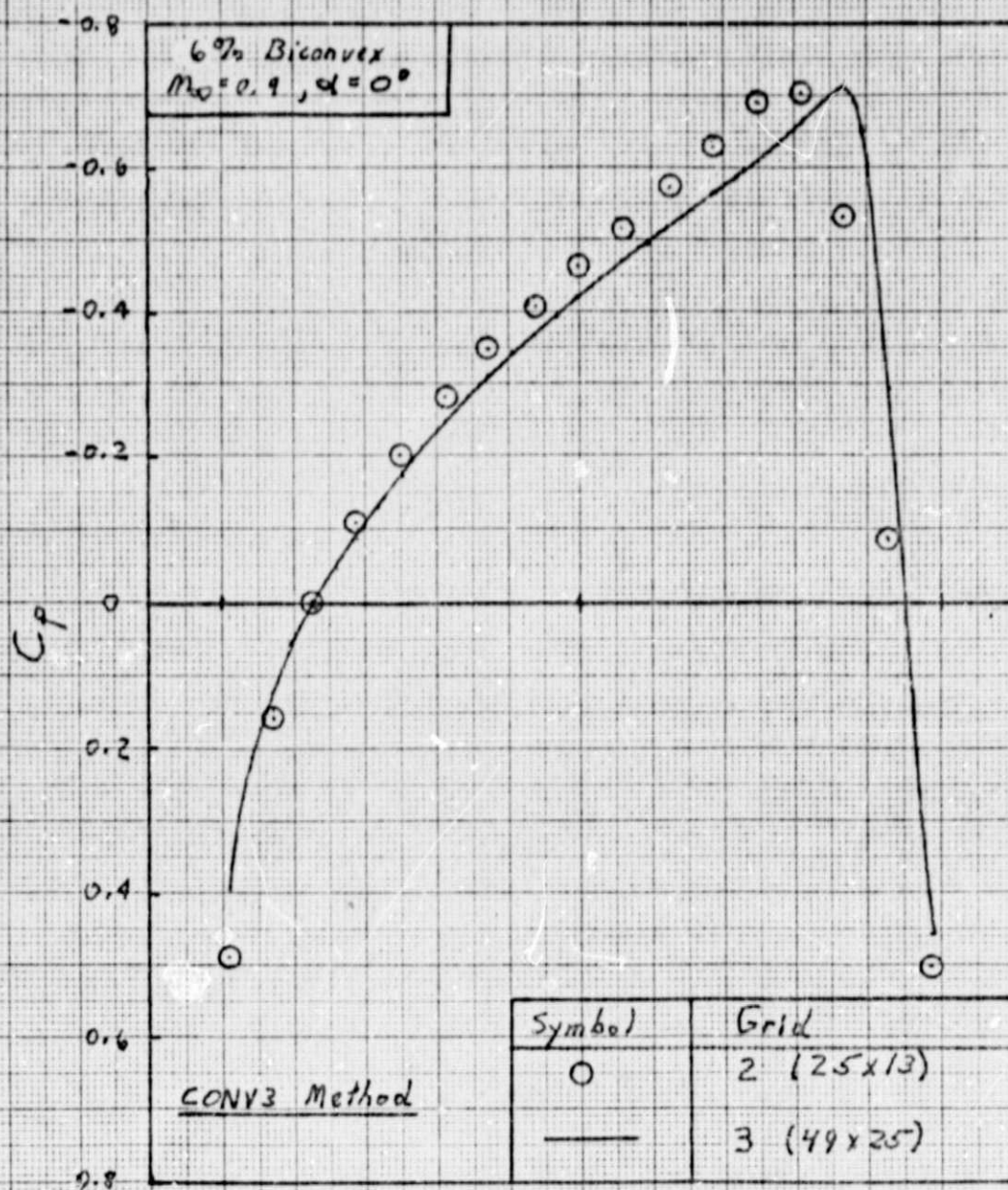


Figure 6. Variation With Grid Size - CONV3 Code

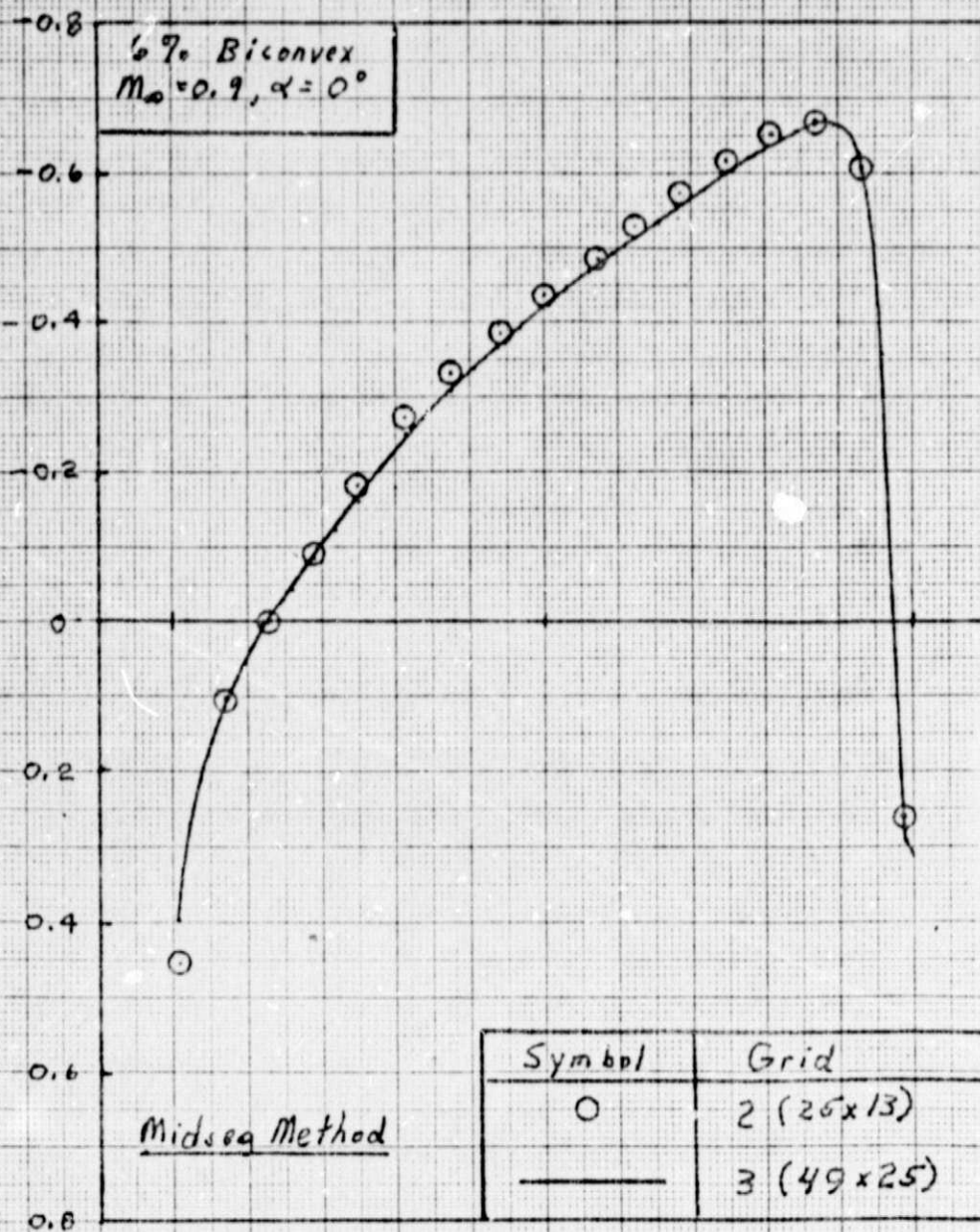


Figure 7. Variation With Grid Size - MIDSEG Code

midsag

(9)